Quantum Electronics **50** (11) 989–994 (2020)

LASERS

https://doi.org/10.1070/QEL17396

Development and study of high-power quantum-cascade lasers emitting at 4.5–4.6 μm

V.V. Dudelev, D.A. Mikhailov, A.V. Babichev, G.M. Savchenko, S.N. Losev, E.A. Kognovitskaya, A.V. Lyutetskii, S.O. Slipchenko, N.A. Pikhtin, A.G. Gladyshev, D.V. Denisov, I.I. Novikov, L.Ya. Karachinsky, V.I. Kuchinskii, A.Yu. Egorov, G.S. Sokolovskii

Abstract. **Quantum-cascade room-temperature 4.5–4.6 μm lasers with different numbers of quantum cascades are developed and studied. It is shown that losses at the metallised sidewalls of the ridge waveguide considerably increase the threshold current density. It is demonstrated that the current density needed to overcome the internal and outcoupling losses in lasers with 30 quantum cascades is an order of magnitude lower than in lasers with 15 quantum cascades.**

Keywords: *quantum-cascade laser, heterostructure, high radiation power.*

1. Introduction

Quantum-cascade lasers (QCLs), due to their compactness and high efficiency, have been extensively studied for almost 50 years. The idea of these lasers was proposed by Suris and Kazarinov as early as in 1971 [1], but one had to wait for more than 20 years for practical realisation of the first functional device [2], which is related first of all to the extremely complicated growth of epitaxial laser structures containing thousands of nanolayers. Intensive studies of QCLs led to development of devices operating at room temperature in the spectral range 3–25 μm [3–6]. Interest to the spectral range 4.5–4.6 μm is explained first all by the fact that this range can be used to detect various materials, in particular, carbon monoxide [7], silane [8], carbon sulphide [9], and nitrogen oxide [10]. At present, there exist QCLs of various designs operating at room temperature in this spectral range. Here we should mention some works devoted to high-power QCLs, both single ridge lasers [11, 12] and devices based on laser bars [13, 14]. It is also necessary to note a progress in the creation of surface-emitting lasers [15, 16], as well as of tunable [17, 18] and single-mode [19, 20] lasers. The QCLs are the key elements of systems for controlling chemicals in the spectral range 4.5–4.6 μm [8–10, 21]. Solution of many problems related to remote detection of chemical materials requires high-power radiation sources, because of which the aim of the present work was to develop and study high-power QCLs for this spectral range.

V.V. Dudelev, D.A. Mikhailov, G.M. Savchenko, S.N. Losev, A.V. Lyutetskii, S.O. Slipchenko, N.A. Pikhtin, V.I. Kuchinskii, G.S. Sokolovskii Ioffe Institute, Politekhnicheskay ul. 26, 194021 St. Petersburg, Russia;
e-mail: gs@mail.ioffe.ru;
A.V. Babichev ITMO University, Kronverkskii prosp. 49, 197101 St. Petersburg, Russia; Connector Optics LLC, ul. Domostroitel'naya 16, 194292 St. Petersburg, Russia;
e-mail: a.babichev@mail.ioffe.ru;
E.A. Kognovitskaya Ioffe Institute, Politekhnicheskay ul. 26, 194021 St. Petersburg, Russia; St. Petersburg Electrotechnical University 'LETI', ul. Prof. Popova 5, 197022 St. Petersburg, Russia;
A.G. Gladyshev Connector Optics LLC, ul. Domostroitel'naya 16, 194292 St. Petersburg, Russia;
D.V. Denisov St. Petersburg Electrotechnical University 'LETI', ul. Prof. Popova 5, 197022 St. Petersburg, Russia;
I.I. Novikov, L.Ya. Karachinsky Ioffe Institute, Politekhnicheskay ul. 26, 194021 St. Petersburg, Russia; ITMO University, Kronverkskii prosp. 49, 197101 St. Petersburg, Russia; Connector Optics LLC, ul. Domostroitel'naya 16, 194292 St. Petersburg, Russia;
e-mail: Leonid.Karachinsky@connector-optics.com;
A.Yu. Egorov ITMO University, Kronverkskii prosp. 49, 197101 St. Petersburg, Russia

Received 4 July 2020; received 7 September 2020
Kvantovaya Elektronika **50** (11) 989–994 (2020)
Translated by M.N. Basieva

2. Development and study of high-power QCLs

The most important problem that sharply decreases the efficiency of 4.5–4.6 μm QCLs based on the $In_{0.53}Ga_{0.47}As/In_{0.52}Al_{0.48}As$ heteropair isoperiodic with the InP substrate is the low height of the potential barrier over the upper quantum-confinement level, which leads to thermal escape of carriers [22]. As was shown in [23], one of the most efficient approaches to solving this problem is the formation of the active QCL region based on strain-compensated heteropairs, which makes it possible to increase the potential barrier over the upper quantum-confinement level of the laser transition by several times. In the present work, we use the strain-compensated $In_{0.67}Ga_{0.33}As/In_{0.36}Al_{0.64}As$ heteropair to form the active region of the QCL. As was shown by calculations, the use of this heteropair makes it possible to increase the conduction band discontinuity at the heterointerface to 800–820 meV, which exceeds the values achievable in the case of using a mechanically unstrained $IIn_{0.53}Ga_{0.47}As/In_{0.52}Al_{0.48}As$ heteropair by 310–320 meV [24]. The thickness of $In_{0.67}Ga_{0.33}As/In_{0.36}Al_{0.64}As$ layers in the quantum cascade was chosen to compensate the mechanical stress and form an elastically balanced hetero-

structure. In this case, the most efficient approach for depopulating the lower laser level is the use of a scheme with two-phonon resonance scattering of charge carriers [25]. Figure 1 presents the calculated profile of the conduction band of a quantum cascade based on the strained $In_{0.67}Ga_{0.33}As/In_{0.36}Al_{0.64}As$ heteropair and the squared wave functions in the cascade layers of the calculated structure. The total quantum cascade thickness was 50.4 nm, and the calculated laser transition energy was 271 meV, which corresponds to the lasing wavelength of 4.57 μm. The calculated lifetimes of caries at the upper and lower levels were $\tau_{up} = 2.6$ ps and $\tau_{low} = 0.39$ ps, respectively. Taking into account the interaction matrix element $z_{up\text{-}low} = 1.91$ nm and the transition time $\tau_{up\text{-}low} = 7.47$ ps, the value characterising the efficiency of the QCL active region design [26] is $z^2_{up-low}\tau_{up}(1-\tau_{low}/\tau_{up\text{-}low}) = 9$ ps nm^2.

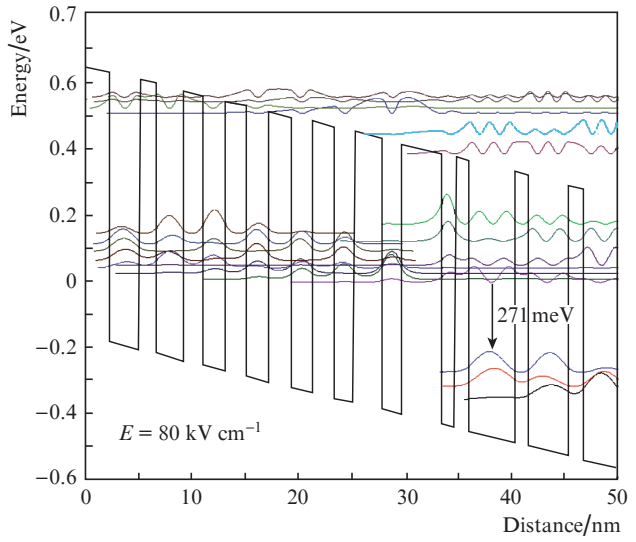

Figure 1. Schematic of the quantum cascade based on the strained $In_{0.67}Ga_{0.33}As/In_{0.36}Al_{0.64}As$ with a calculated conduction band profile and squared electron wave functions in the quantum cascade layers at an electric field strength of 80 kV cm^{-1}. The arrow indicates the laser transition.

As is known, to obtain a high output laser power, it is important to decrease the internal optical losses. One of the sources of these losses is the absorption at the upper metal contact and the near-contact heavily doped region. It is obvious that the free-carrier absorption can be decreased by increasing the thickness of the weakly doped upper waveguide cladding. However, this leads to an increase in the device resistance and, as a result, to higher losses. Thus, as is shown in Fig. 2, there exists an optimal thickness of the upper cladding depending on the thickness of the QCL active region (on the number of quantum cascades in the structure).

Based on performed investigations, we have grown QCL heterostructures containing 15 quantum cascades in the active region (Table 1) by molecular-beam epitaxy at the Connector Optics LLC on a Riber 49 production system.

After the growth, ridges on the QCL heterostructures were formed by etching deep trenches. For this purpose, the planar structure surface was covered with a S1813

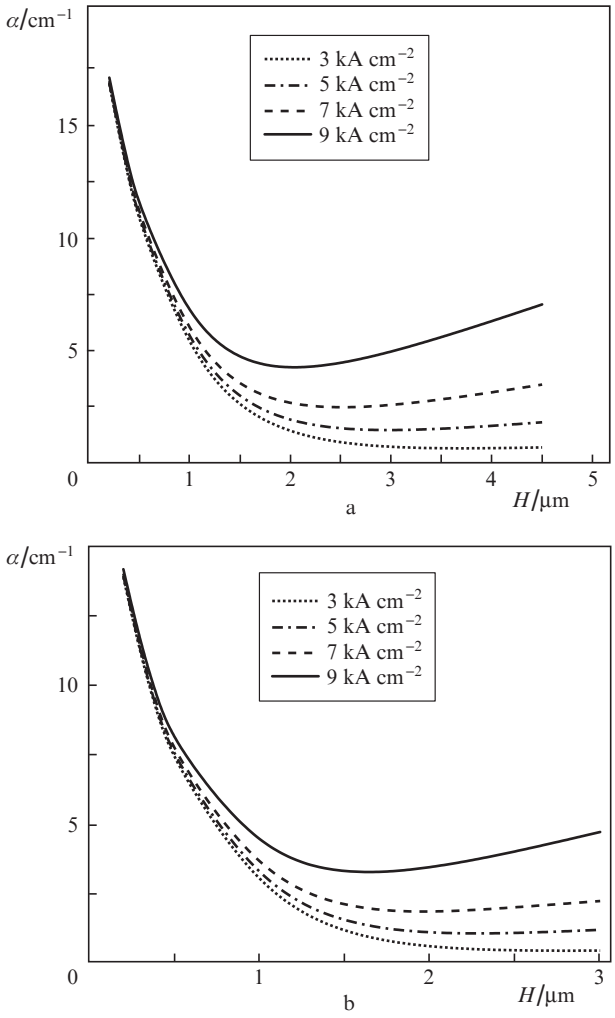

Figure 2. Calculated dependences of the optical total losses in a QCL waveguide on the thickness of the weakly doped upper waveguide cladding in the case of (a) 15 and (b) 30 cascades at different current densities.

Table 1. QCL heterostructure with 15 quantum cascades based on the $In_{0.67}Ga_{0.33}As/In_{0.36}Al_{0.64}As$ heteropair in the active region.

Material	Layer type	Thickness/ μm	Doping level/ cm^{-3}
$In_{0.53}Ga_{0.47}As$	Contact layer	0.2	2.5×10^{19}
InP	Contact layer	0.2	1.0×10^{19}
InP	Near-contact layer	0.5	7.0×10^{18}
InP	Upper waveguide cladding	3.5	1.0×10^{17}
15 quantum cascades	Active region	0.756	2.7×10^{16}
InP	Lower waveguide cladding	0.3	1.0×10^{17}
InP	Substrate	350	3.0×10^{17}

photoresist mask in the form of parallel windows 11 μm wide. Wet etching thought the photoresist mask was performed to a depth exceeding the heterostructure thickness by 1–2 μm using a nonselective etching solution $HBr:HCl:H_2O_2:H_2O = 10:5:1:50$. Then, a SiO_2 dielectric

layer was deposited by plasma-enhanced chemical vapour deposition. Opening of windows in the dielectric on the top of the ridge waveguide formed by the trenches was performed by etching in a buffered etching solution through a photoresist mask (photoresist AZ4533) covering the trenches, edges of ridges, and the planar surface between ridges. The image of a ridge with deposited dielectric and an opened window for the ohmic contact is shown in Fig. 3.

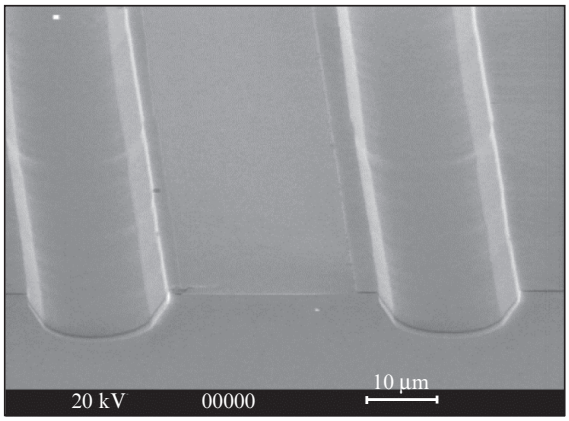

a

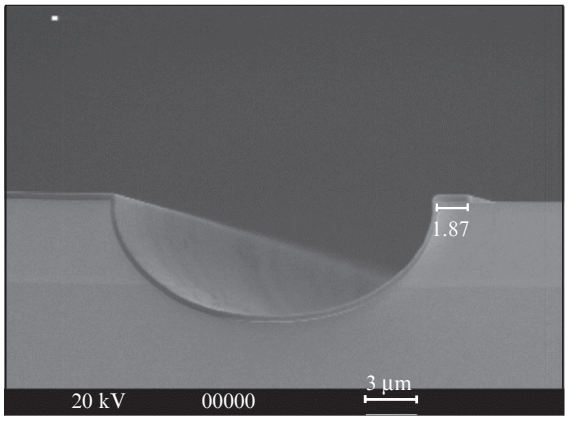

b

Figure 3. SEM images of a ridge with dielectric deposited on the sidewalls: (a) general image of a ridge formed by deep trenches and (b) magnified image of one of the ridge sidewalls.

After deposition of the upper contact, lapping of the substrate, and deposition of the lower contact, the heterostructure was cleaved into chips ~3 mm long. We studied QCLs with the ridge contact width $W = 10–50$ μm. The lasers were mounted on a primary heat sink with the heterostructure down to provide efficient heat removal from the active region of the QCL.

The fabricated QCLs were studied in a pulsed regime. The current pulse duration was ~75 ns at a repetition rate of 48 kHz. All the studied lasers operated at room temperature.

Investigations of the spectral characteristics of the QCLs (Fig. 4) showed that lasing at room temperature occurs near 4.5 μm, which corresponds to preliminary theoretical estimates made in [24]. The spectra were measured using an MDR-23 monochromator with a 150-mm^{-1} diffraction grating and a Vigo Systems PVI-4TE-10.6 photodetector. The measurement technique is described in more detail in [27, 28].

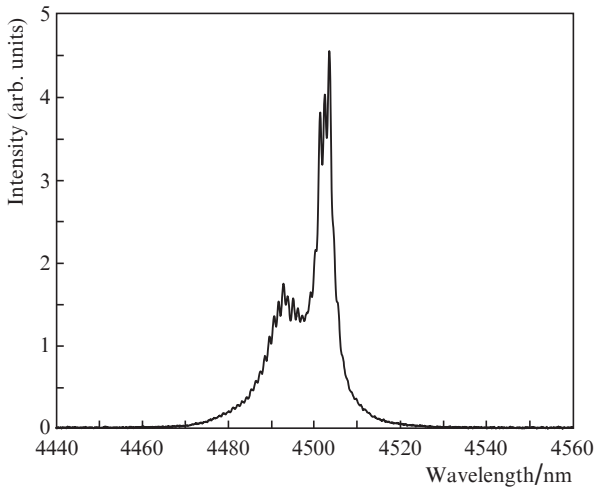

Figure 4. Typical spectrum of a QCL with 15 quantum cascades in the active region and a ridge contact width $W = 50$ μm at a current of 9 A ($1.25I_{th}$).

The power characteristics of QCLs were studied in a pulsed regime as was described in detail in [29]. Typical light–current characteristics of QCLs with ridge contact widths $W = 10$, 16, 20, and 50 μm are presented in Fig. 5. The maximum output optical peak power of the studied QCLs did not exceed 0.5 W (~0.25 W from one facet). The observed slope oefficiency increased with increasing W, namely, this slope was 0.26 W A^{-1} for the QCL with $W = 16$ μm and even 0.35 W A^{-1} for the QCL with $W = 50$ μm.

Study of the threshold characteristics of QCLs allowed us to estimate the influence of optical losses at the sidewalls of the ridge waveguide on the QCL threshold current. Figure 6 shows the measured dependence of the QCL threshold current I_{th} on the ridge contact width W. One can see that the threshold current linearly decreases with decreasing W. The

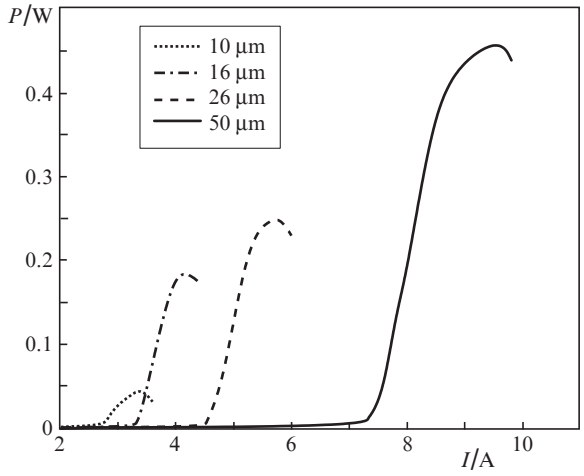

Figure 5. Typical light–current characteristics of QCLs with 15 quantum cascades in the active region and ridge contact widths $W = 10$, 16, 26, and 50 μm.

linear approximation of this dependence (solid line *1* in Fig. 6) shows that a considerable fraction of the current is spent for overcoming the losses at the mesa periphery: the threshold current at W tending to zero is ~1.65 A.

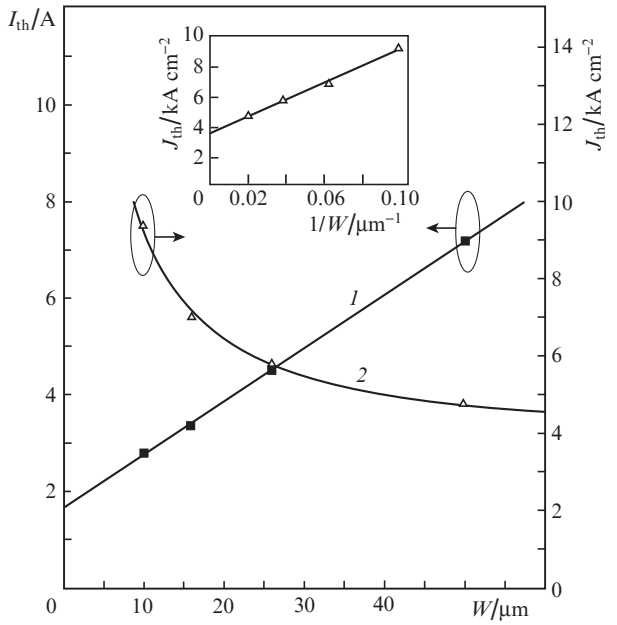

Figure 6. Dependences of threshold current I_{th} and threshold current density J_{th} of a QCL with 15 quantum cascades in the active region on the ridge contact width W. Squares and triangles are the experimental values of threshold currents and threshold current densities, respectively; curve (*1*) is the linear approximation of the dependence of I_{th} on W; and curve (*2*) is the hyperbolic approximations of the dependence of J_{th} on W. The inset shows the dependence of J_{th} on W^{-1}.

Figure 3 shows that the obtained ridge waveguides have a high quality, which allows us to conclude that the source of losses is the absorption of light in metal due to penetration of the side mode through the dielectric layer to the metallised layers of the sidewalls rather than the scattering of light at the waveguide sidewalls. The dependence of the threshold current density J_{th} on the contact width W presented in Fig. 6 corresponds to the hyperbolic approximation of the dependence of J_{th} on W. The limit of this dependence at an infinitely large width W is the current density required to overcome the internal and outcoupling losses without allowance for losses at the sidewalls, which is determined at the point of intersection of the linear approximation of $J_{th}(1/W)$ with the ordinate axis, i.e., at $1/W = 0$ (see the inset in Fig. 6). The obtained high current density necessary for overcoming the internal and outcoupling losses (~3.6 kA cm^{-2}) for QCLs with 15 quantum cascades in the active region, as well as the high fraction of the threshold current related to losses at the sidewalls of the ridge waveguide, indicate that it is necessary to introduce changes in the active region of the QCL and increase the gain.

Taking all these facts into account, we fabricated a new QCL structure with quantum cascades based on the strain-compensated $In_{0.67}Ga_{0.33}As/In_{0.36}Al_{0.64}As$ heteropair with a number of quantum cascades increased to 30 (Table 2).

The post-growth treatment of these heterostructures is similar to the procedure described above. We have fabricated QCLs with ridge contact widths of 16–50 μm and a cavity length of 3 mm.

Table 2. QCL heterostructure with 30 quantum cascades based on the $In_{0.67}Ga_{0.33}As/In_{0.36}Al_{0.64}As$ heteropair in the active region.

Material	Layer type	Thickness/ μm	Doping level/ cm^{-3}
$In_{0.53}Ga_{0.47}As$	Contact layer	0.2	2.5×10^{19}
InP	Near-contact layer	1.0	2.0×10^{18}
InP	Upper waveguide cladding	2.0	1.0×10^{17}
30 quantum cascades	Active region	1.512	2.7×10^{16}
InP	Lower waveguide cladding	0.3	1.0×10^{17}
InP	Substrate	350	3.0×10^{17}

The QCLs with the active region containing 30 quantum cascades were studied at room temperature under the same conditions as in the case of QCLs with 15 quantum cascades. Investigations of the dependences of I_{th} and J_{th} on W (Fig. 7) showed an approximately 25% decrease in the current required to overcome the losses at the sidewalls of the ridge waveguide, i.e., a decrease to 1.22 A from 1.65 A for QCLs with 15 quantum cascades. In addition (see the inset in Fig. 7), the threshold current density needed to overcome the internal and outcoupling losses for QCLs with 30 quantum cacscades decreased almost by an order of magnitude, i.e., to 0.44 kA cm^{-2} in comparison with 3.6 kA cm^{-2} for QCLs with 15 quantum cascades. All this opens the possibility of obtaining cw lasing at room temperature by optimising the post-growth treatment of heterostructures and decreasing the losses in the laser waveguide.

In addition, investigations of the spectral characteristics of QCLs with 30 quantum cascades in the active region showed that their spectrum is considerably broader than the spectrum of QCLs with 15 quantum cascades, which can be caused by a higher gain in the active region based on 30 cascades. A typical spectrum of such a QCL is given in Fig. 8.

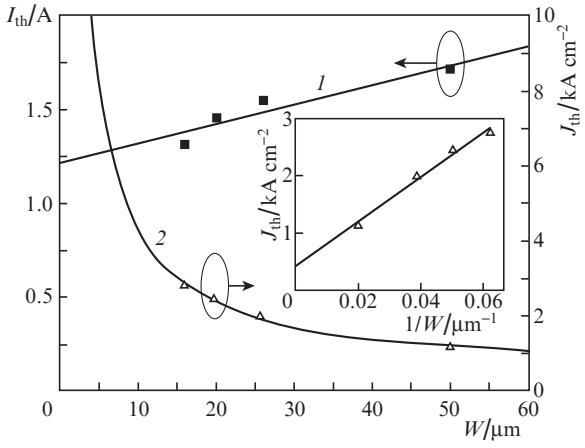

Figure 7. Dependences of threshold current I_{th} and threshold current density J_{th} of a QCL with 30 quantum cascades in the active region on the ridge contact width W. Squares and triangles are the experimental values of threshold currents and threshold current densities, respectively; curve (*1*) is the linear approximation of the dependence of I_{th} on W; and curve (*2*) is the hyperbolic approximations of the dependence of J_{th} on W. The inset shows the dependence of J_{th} on W^{-1}.

As is seen from the spectra shown in Figs 4 and 8, at comparable levels with respect to the lasing threshold, the spectrum of a QCL with a Fabry–Perot cavity broadens almost fivefold as the number of quantum cascades increases from 15 to 30.

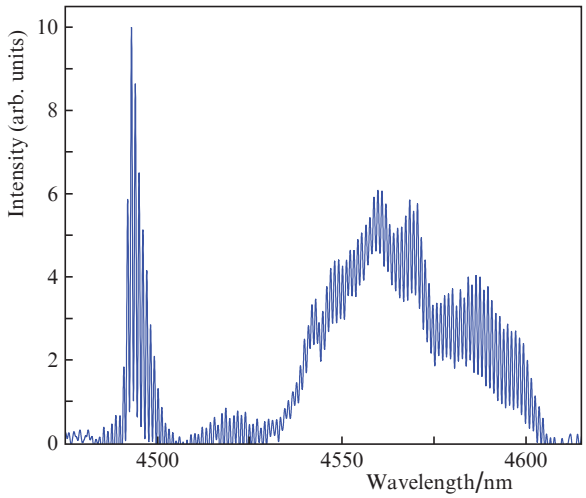

Figure 8. Typical spectrum of a QCL with 30 cascades in the active region and a ridge contact width of 50 μm at a pump current of 4.6 A ($1.25I_{th}$).

Typical light–current characteristics of QCLs with 30 quantum cascades in the active region and stripe contact widths of 16, 20, 26, and 50 μm are presented in Fig. 9. One can see that an increase in the number of cascades in the QCL active region from 15 to 30 allowed us to increase the output power by an order of magnitude at identical geometrical dimensions. The maximum output optical power of QCLs with $L = 3$ mm and $W = 50$ μm was ~5 W (~2.5 W from one facet). The slope of the light–current characteristic for these QCLs decreased with increasing W. The maximum slope efficiency reached 1.78 W A^{-1} for lasers with $W = 16$ μm and 1.35 and 1.3 W A^{-1} for lasers with W of 20 and 50 μm, respectively. An exception were lasers with $W = 26$ μm, whose light–current characteristic had a slope lower than 1 W A^{-1}, which is obviously related to a poorer quality of the post-growth treatment of this QCL series. The maximum obtained slope efficiency of the light–current characteristic of QCLs with 30 cascades in the active region is almost five times higher than that of QCLs with 15 cascades. An increase in the cavity length to 5 mm allowed us to obtain the maximum output optical power exceeding 10 W (more that 5 W from one facet, Fig. 9) [30] at a slope efficiency of the light–current characteristic of 1.15 W A^{-1}.

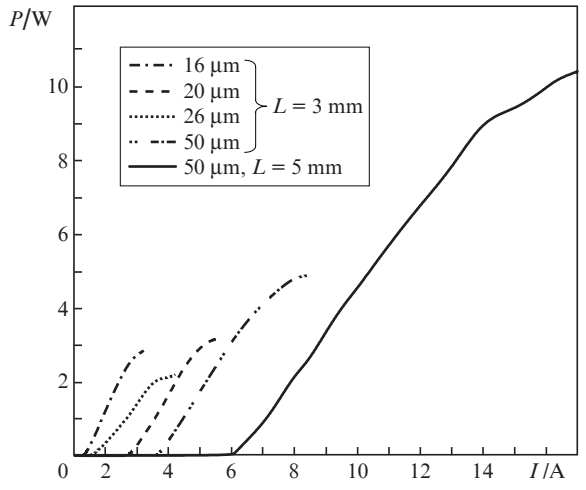

Figure 9. Light–current characteristics of QCLs with 30 cascades in the active region, $W = 10$, 16, 26, and 50 μm, and cavity length $L = 3$ mm, as well as with $W = 50$ μm and $L = 5$ mm.

3. Conclusions

Thus, we developed and studied high-power 4.5–4.6-μm QCLs with different numbers of quantum cascades operating at room temperature. It is shown that the optical losses at the metallised sidewalls of the ridge waveguide considerably increase the threshold current density. It is demonstrated that the current density necessary to overcome the internal and outcoupling losses in QCLs with 30 quantum cascades decreases almost by an order with respect to that for QCLs with 15 cascades, i.e., it is 0.44 and 3.6 kA cm^{-2} for QCLs with 30 and 15 cascades, respectively. The increase in the number of cascades in the active region of QCLs from 15 to 30 allowed us to increase the output optical power by an order of magnitude for lasers with identical geometrical dimensions. In particular, the maximum output optical power for a QCL with a cavity length of 3 mm and a ridge contact width of 50 μm was about 5 W (~2.5 W from one facet), while the corresponding output optical power in the case of a cavity length of 5 mm exceeded 10 W (more than 5 W from one facet). It is noted that it is possible to achieve continuous-wave lasing at room temperature by optimising the post-growth treatment of heterostructures and decreasing losses in the laser waveguide.

Acknowledgements. This work was supported by the Ministry of Science and Higher Education of the Russian Federation (unique identifier RFMEFI60719X0318).

References

1. Kazarinov R.F., Suris R.A. *Semiconductors*, **5**, 707 (1971) [*Fiz. Tekhn. Poluprovodn.*, **5**, 797 (1971)].
2. Faist J., Capasso F., Sivco D.L., Hutchinson A.I., Cho A.Y. *Science*, **264**, 553 (1994).
3. Dudelev V.V., Mikhailov D.A., Babichev A.V., Andreev A.D., Losev S.N., Kognovitskaya E.A., Bobretsova Yu.K., Slipchenko S.O., Pikhtin N.A., Gladyshev A.G., Denisov D.V., Novikov I.I., Karachinsky L.Ya., Kuchinskii V.I., Egorov A.Yu., Sokolovskii G.S. *Quantum Electron.*, **50**, 141 (2020) [*Kvantovaya Elektron.*, **50**, 141 (2020)].
4. Botez D., Chang C.-C., Mawst l.J. *J. Phys. D: Appl. Phys.*, **49**, 043001 (2016).
5. Babichev A.V., Gladyshev A.G., Kurochkin A.S., Dudelev V.V., Kolodeznyi E.S., Sokolovskii G.S., Bugrov V.E., Karachinsky L.Ya., Novikov I.I., Denisov D.V., Ionov A.S., Slipchenko S.O., Lyutetskii A.V., Pikhtin N.A., Egorov A.Yu. *Tech. Phys. Lett.*, **45**, 398 (2019) [*Pis'ma Zh. Tekh. Fiz.*, **45** (8), 31 (2019)].
6. Loghmari Z., Bahriz M., Meguekam A., Teissier R., Baranov A.N. *Electron. Lett.*, **55**, 144 (2019).
7. Curl R.F., Capasso F., Gmachl C., Kosterev A.A., McManus B., Lewicki R., Pusharsky H., Wysocki G., Tittel F. *Chem. Phys. Lett.*, **487**, 1 (2010).

8. Man Helden J.H., Lopatik D., Navea A., Lang N., Davies P.B., Röpcke J. *J. Quant. Spectrosc. Radiat. Transfer*, **151**, 287 (2015).
9. Yang C.G., Deng H., Qian Y.Y., Li M.X., Chen B., Xu Z.Y., Kan R.F. *Spectrochim. Acta Pt A: Molec. Biomolec. Spectrosc.*, **225**, 117478 (2020).
10. Zhou S., Liu N.W., Zhang L., He T.B., Li J.S. *Spectrochim. Acta Pt A: Molec. Biomolec. Spectrosc.*, **205**, 79 (2018).
11. Semtsiv M.P., Masselink W. *Appl. Phys. Lett*., **109**, 203502 (2016).
12. Liang P., Liu F.Q., Zhang J.C., Wang L.J., Liu J.Q., Wang Z.G. *Chin. Phys. Lett*., **29**, 074215 (2012).
13. Yan F.-L., Zhang J.-C., Jia Z.-W., Zhuo N., Zhai S.-Q., Liu S.-M., Liu F.-Q., Wang Z.-G. *AIP Advances*, **6**, 035022 (2016).
14. Lyakh A., Maulini R., Tsekoun A., Go R., Kumar C., Patel N. *Opt. Express*, **22**, 1203 (2014).
15. Yao D.-Y., Zhang J.-C., Liu F.-Q., Zhuo N., Yan F.-L., Wang L.-J., Liu J.-Q., Wang Z.-G. *Appl. Phys. Lett*., **103**, 041121 (2013).
16. Yao D.-Y., Zhang J.-C., Liu F.-Q., Jia Z.-W., Yan F.-L., Wang L.-J., Liu J.-Q., Wang Z.-G. *IEEE Photonics Technol. Lett*., **26**, 323 (2014).
17. Zhang J.-C., Wang L.-J., Liu W.-F., Liu F.-Q., Yin W., Liu J.-Q., Li L., Wang Z.-G. *Chin. Phys. Lett*., **28**, 074203 (2011).
18. Dhirhe D., Slight T.J., Nshii C.C., Ironside C.N. *Semicond. Sci. Technol*., **27**, 094007 (2012).
19. Zhang J.C., Liu F.Q., Tan S., Yao D.Y., Wang L.J., Li L., Liu J.Q., Wang Z.G. *Appl. Phys. Lett*., **100**, 112105 (2012).
20. Zhang J.C., Wang L.J., Chen J.Y., Zhao L.H., Liu F.Q., Liu, J.Q., Wang Z.G. *Electron. Lett*., **47**, 1338-U56 (2011).
21. Nwaboh J.A., Persijn S., Arrhenius K., Bohlén H., Werhahn O., Ebert V. *Meas. Sci. Technol*., **29**, 095010 (2018).
22. Lyakh A., Maulini R., Tsekoun A., Go R., Von der Porten S., Pflugl C., Diehl L., Capasso F., Patel C.K.N. *Proc. Natl. Acad. Sci*., **107**, 18799 (2010).
23. Egorov A.Yu., Babichev A.V., Karachinsky L.Ya., Novikov I.I., Nikitina E.V., Chernyshova M., Sofronov A.N., Firsov D.A., Vorob'ev L.E., Pikhtin N.A., Tarasov I.S. *Semiconductors*, **49**, 1527 (2015) [*Fiz. Tekhn. Poluprovodn*., **49**, 1574 (2015)].
24. Babichev A.V., Gladyshev A.G., Dyudelev V.V., Karachinsky L.Ya., Novikov I.I., Denisov D.V., Slipchenko S.O., Lyutetskii A.V., Pikhtin N.A., Sokolovskii G.S., Egorov A.Yu. *Tech. Phys. Lett*., **46**, 444 (2020) [*Pis'ma Zh. Tekh. Fiz*., **46** (9), 35 (2020)].
25. Hofstetter D., Beck M., Aellen T., Faist J. *Appl. Phys. Lett*., **78**, 396 (2001).
26. Rajeev A., Sigler C., Earles T.L., Flores Y.V., Mawst L.J., Botez D. *Opt. Eng*., **57**, 011017 (2017).
27. Dyudelev V.V., Losev S.N., Myl'nikov V.Yu., Babichev A.V., Kognovitskaya E.A., Slipchenko S.O., Lyutetskii A.V., Pikhtin N.A., Gladyshev A.G., Karachinsky L.Ya., Novikov I.I., Egorov A.Yu., Kuchinskii V.I., Sokolovskii G.S. *Tech. Phys. Lett*., **63**, 1656 (2018) [*Pis'ma Zh. Tekh. Fiz*., **88**, 1708 (2018)].
28. Dudelev V.V., Losev S.N., Myl'nikov V.Yu., Babichev A.V., Kognovitskaya E.A., Slipchenko S.O., Lyutetskii A.V., Pikhtin N.A., Gladyshev A.G., Karachinsky L.Ya., Novikov I.I., Egorov A.Yu., Kuchinskii V.I., Sokolovskii G.S. *Opt. Spectrosc*., **125**, 402 (2018) [*Opt. Spektrosk*., **125**, 387 (2018)].
29. Babichev A.V., Dyudelev V.V., Gladyshev A.G., Mikhailov D.A., Kurochkin A.S., Kolodeznyi E.S., Bugrov V.E., Nevedomskii V.N., Karachinsky L.Ya., Novikov I.I., Denisov D.V., Ionov A.S., Slipchenko S.O., Lyutetskii A.V., Pikhtin N.A., Sokolovskii G.S., Egorov A.Yu. *Tech. Phys. Lett*., **45**, 735 (2019) [*Pis'ma Zh. Tekh. Fiz*., **45** (14), 48 (2019)].
30. Dudelev V.V., Mikhailov D.A., Babichev A.V., Losev S.N., Kognovitskaya E.A., Lyutetskii A.V., Slipchenko S.O., Pikhtin N.A., Gladyshev A.G., Denisov D.V., Novikov I.I., Karachinsky L.Ya., Kuchinskii V.I., Egorov A.Yu., Sokolovskii G.S. *Quantum Electron*., **50**, 720 (2020) [*Kvantovaya Elektron*., **50**, 720 (2020)].